INTERNATIONAL JOURNAL OF INFORMATION SECURITY SCIENCE
E. Şahin, Vol.12, No.1, pp.1-12.
https://doi.org/10.55859/ijiss.1210521

Realization of Quantum Mean Filters with Different Sized on NEQR Quantum Images by QFT Based Operations

Engin Şahin

Department of Computer Engineering, Faculty of Engineering
Çanakkale Onsekiz Mart University
Çanakkale, Turkey
Corresponding Author: enginsahin@comu.edu.tr

Research Paper Received: 26.11.2022 Revised: 08.01.2023 Accepted: 09.01.2023

Abstract—For some image processing algorithms such as edge detection and segmentation, filtering in the spatial domain is an important pre-processing to improve the quality of the image by removing the noise in the images. The time and memory requirements for processing also increase as the size of the images increases. Besides, excessive blurring of the image during noise removal operation can lead to excessive deterioration of image quality. Therefore, the balance between noise reduction and blur needs to be well adjusted. In this paper, a new quantum method for noise reduction on quantum images using QFT-based arithmetic operators is proposed and quantum circuits are designed. Mean filtering operators of different sizes are used to remove noise. First, the classical image is represented by the gray scale quantum image model, the novel enhanced quantum representation (NEQR) model. A quantum method is proposed and circuits are presented for the realization of Mean filters of different sizes on the basis of addition and division operations. Finally, the performance of the method is evaluated by presenting the circuit complexity of the method and the simulation results. In the proposed method, it is aimed to use less resources and reduce the circuit complexity. The optimal filtering operator size is investigated for the balance between noise reduction and image blur.

Keywords—quantum computing, quantum image processing, noise reduction, image smoothing, mean filter

1. Introduction

Quantum computing provides a significant acceleration and security in solving problems compared to classical methods [1], [2], [3]. Quantum computing uses the features of the quantum mechanics such as superposition and entanglement, thus, provides advantages in terms of time and security [4], [5]. Scientists are developing quantum algorithms to process big data faster and make it more secure in the field of informatics. Quantum computing will be an important tool for researchers in many fields, especially physics, chemistry, engineering and medicine [4]. Image processing, which is used in almost every field today, is one of the most important study subjects.

Due to the increase in the details of features

such as resolution, number of channels and depth in imaging devices, the sizes of the images are also getting larger. As such, the time required for processing on these large images also increases. On the basis of the principles of quantum computing, especially superposition and entanglement, the operations in image processing can be accelerated with the quantum methods. In quantum image processing, classical images are represented as quantum states in a related quantum image representation model, quantum processes are applied to these quantum states, and finally, the processed classical image is obtained by quantum measurement. There are many quantum image representation models in the literature for different image types and purposes.

Quantum image representation models are divided into two according to the encoding of color information. The first group encodes the color information to the amplitude or angle of the qubit. The most prominent of the models in this group are the Flexible Representation of Quantum Images (FRQI) [6] which represent single-channel images and the Multi-Channel Representation for Quantum images (MCQI) [7] which represent three-channels (RGB) images. The second group encodes the color information to the basis states of the qubit sequence. The most prominent of the models in this group are the Novel Enhanced Quantum Representation (NEQR) [8] for single-channel images, the Novel Quantum Representation of Color Digital images (NCQI) [9] for three-channels (RGB) images and the Quantum Representation of Multi-Wavelength images (QRMW) [10] for multi-wavelength images. Other quantum image representation models are listed and summarized in Ref. [11]. Many quantum image processing algorithms have been developed based on these representation models, please refer to Refs. [12], [5] for such algorithms.

Image filtering is an important step for noise reduction and image enhancement. In the literature, there are very few studies on noise reduction or image smoothing operations with quantum image filtering. Lomont [13] proposed that quantum convolution and quantum correlation algorithms are physically impossible to implement. Yuan et al. [14] presented quantum image filtering in the spatial domain for NEQR images. Although the quantum correlation of the two sequences is physically impossible to implement, they proved that it can be achieved with the high quantum parallel method to correlate the image and filter mask. The mean filter as a filter is used, ignoring $1/9$. In this method, the filter values must be integers and must be known before applying. Yuan et al. [15] improved the quantum image filtering in the spatial domain. The two shortcomings in the previous work were overcome by using quantum multiplication instead of quantum addition. Li et al. [16] designed the quantum weighted average filter by investigating spatial filtering. Quantum circuits are designed with some auxiliary modules for the arithmetic operations and the weighted averaging filter of size 3×3 to be used in noise removal applications on the images. Quantum superposition is not used in this study and therefore many ancillary qubits are required [18]. Li et al. [17] performed the quantum median filter in the spatial domain, then improved the method in terms of noise removal and complexity in Ref. [12]. Ali et al. [18] proposed a new approach using a modular design procedure for the quantum mid-point filter, which specifically reduces the number of ancillary qubits. They also proposed a method that creates only one copy of the positional information in the process of creating multiple copies of the image. Şahin and Yilmaz [5] applied smoothing filters using QFT-based operators on the QRMW model [10] to remove noise in the multi-wavelength images before edge detection operation. A generalized method for applying any

filter operator is presented.

In this study, realization of quantum mean filters with different sized on NEQR quantum images by QFT-based operations is proposed. The NEQR model is used in this study because it requires fewer qubits for single-channel images than the QRMW model. Advantages in speed and resource usage With using the QFT-based operators are obtained by reducing circuit complexity and using fewer ancillary qubits. In order to further reduce the circuit complexity and the number of qubits used, a specific method to the relevant filtering mask operator is presented instead of the generalized method in [5] with QFT-based operators. In order to apply the Mean filter algorithm in different sized, addition and division operations is used instead of multiplication for reducing complexity and speed up. The algorithm and quantum circuits of the proposed method are presented. Simulations and analyzes are realized by using filters of different sized on different images, and the efficiency of the method is demonstrated by presenting the results. The advantages of the quantum method over the classical method are also discussed.

This paper is organized as follows: Section 2 briefly introduces some preliminary information about the NEQR, applying Mean filter and the QFT based arithmetic operators used in this study. In Section 3,we present the quantum mean filters with different sized on the NEQR image model and the quantum circuits used in the algorithm. Section 4 analyses complexity and simulation results, gives the discussion. Section 5 provides a conclusion and future works proposal of the paper.

2. Preliminaries

In this section, we briefly introduce some preliminary information about the NEQR model, the Mean filter and the QFT-based quantum arithmetic operations.

2.1. NEQR

The basis states of qubit sequence are used to store the color and position information of image in the NEQR model [8]. The NEQR model represents only gray-scale images. Suppose the gray scale of image is 2^q. The binary sequence $C_{YX}^0 C_{YX}^1 ... C_{YX}^{q-2} C_{YX}^{q-1}$ encodes the gray-scale value $f(Y,X)$ of the corresponding pixel (Y,X) as follows [8]:

$$\begin{aligned} f\left(Y,X\right) &= C_{YX}^0 C_{YX}^1 ... C_{YX}^{q-2} C_{YX}^{q-1}, \\ C_{YX}^k \in [0,1], \quad & f\left(Y,X\right) \in [0, 2^q - 1]. \end{aligned} \tag{1}$$

The quantum state of a image for a $2^n \times 2^n$ image can be written as follows [8]:

$$\begin{aligned} |I\rangle &= \frac{1}{2^n} \sum_{Y=0}^{2^n-1} \sum_{X=0}^{2^n-1} |f\left(Y,X\right)\rangle |YX\rangle \\ &= \frac{1}{2^n} \sum_{Y=0}^{2^n-1} \sum_{X=0}^{2^n-1} \bigotimes_{i=0}^{q-1} |C_{YX}^i\rangle |YX\rangle . \end{aligned} \tag{2}$$

A sample of a $2^n \times 2^n$ gray image and its quantum state $|I\rangle$ in the NEQR model are shown in Figure 1 and (3), respectively.

$$\begin{aligned} |I\rangle = \; & |00000000\rangle |0000\rangle + |00001010\rangle |0001\rangle + \\ & |00011110\rangle |0010\rangle + |00110010\rangle |0011\rangle + \\ & |01000110\rangle |0100\rangle + |01011010\rangle |0101\rangle + \\ & |01101110\rangle |0110\rangle + |10000010\rangle |0111\rangle + \\ & |10010110\rangle |1000\rangle + |10101010\rangle |1001\rangle + \\ & |10111110\rangle |1010\rangle + |11010010\rangle |1011\rangle + \\ & |11011100\rangle |1100\rangle + |11100110\rangle |1101\rangle + \\ & |11110000\rangle |1110\rangle + |11111111\rangle |1111\rangle . \end{aligned} \tag{3}$$

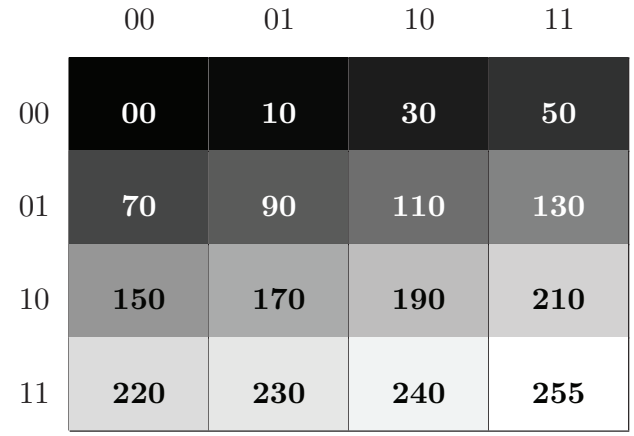

Figure 1. A sample of a $2^n \times 2^n$ gray image.

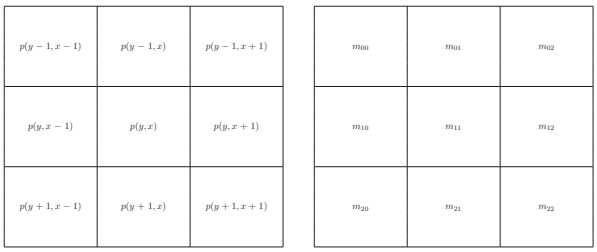

Figure 2. The inner product matrices (a) the partial matrix (P) (b) the filter mask operator matrix (M) (adapted from [5]).

2.2. Mean filter

Spatial filtering is based on processing a pixel in the image with the filtering mask operator associated with its neighboring pixels [16]. The result value of the filtering operation is treated as the new value of the relevant pixel. The smoothing linear filters which are also referred to low-pass filters (LFP) are used commonly for smoothing the image [5]. According to the size of the filter mask operator to be applied, the result (V) of the inner product of the partial matrix (P) formed by the relevant pixel (y, x) and its neighbor pixels and the filter mask matrix (M) is considered as the new value of the relevant pixel (y, x). The result of inner product (V) of the two 3×3 matrices (P, M) shown in Figure 2 is given as follows:

$$\begin{aligned} V = \; & m_{00} \times p(y-1, x-1) + m_{01} \times p(y-1, x) + \\ & m_{02} \times p(y-1, x+1) + m_{10} \times p(y, x-1) + \\ & m_{11} \times p(y, x) + m_{12} \times p(y, x+1) + \\ & m_{20} \times p(y+1, x-1) + m_{21} \times p(y+1, x) + \\ & m_{22} \times p(y+1, x+1). \end{aligned} \tag{5}$$

The 3×3 dimensional version of the mean filter operator is given in Figure 3. In this study, instead of doing the inner product with decimal numbers as in Figure 3a, the filter is applied by adding and dividing with integers instead of multiplying with decimals, considering as in Figure 3b.

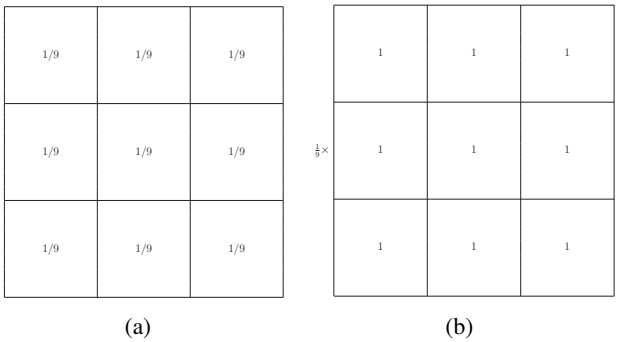

Figure 3. The mean filter operator values (a) decimal (b) integer.

$$\text{innerproduct}: \; \mathbf{P} \cdot \mathbf{M} = \sum_{i=0}^{2} \sum_{j=0}^{2} P_{ij} M_{ij}. \tag{4}$$

2.3. QFT-based quantum arithmetic operations

The arithmetic operators based on classical computation used in the existing studies [14], [15], [16], [17], [12], [18] in the literature only operate on non-negative integers. In this study, QFT-based quantum arithmetic operators [19], [3] that can perform both modular and non-modular operations on all integers are used. The quantum circuits of the non-modular arithmetic operations used in the study are given in Figure 4 as simplified graphs, please refer to [19], [3] for details of quantum circuits and operations. The cyclic shift transformation operators C_{x+} and C_{x-} on the x-axis, C_{y+} and C_{y-} on the y-axis presented by Le et al. [20] are used for the shifting process. The quantum circuits of the transformations operators C_{x+} and C_{x-} are shown in Figure 5.

The $|x\rangle$ and $|y\rangle$ in quantum circuits represent the quantum states of the signed integers n-bit x and m-bit y and the quantum states are given as follows.

$$|x\rangle = |x_0 x_1 \cdots x_{n-1}\rangle = |x_0\rangle \otimes |x_1\rangle \otimes \cdots \otimes |x_{n-1}\rangle \quad (6)$$

$$|y\rangle = |y_0 y_1 \cdots y_{m-1}\rangle = |y_0\rangle \otimes |y_1\rangle \otimes \cdots \otimes |y_{m-1}\rangle \quad (7)$$

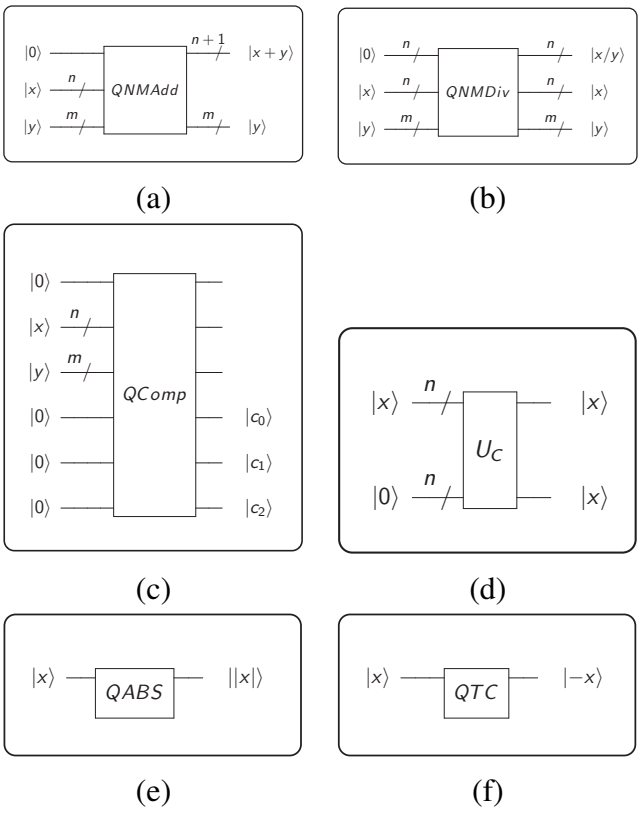

Figure 4. The quantum circuits of the QFT based non-modular arithmetic operations (a) Addition as $QNMAdd$ (b) Division as $QNMDiv$ (c) Comparator as $QComp$ (d) Copy as U_C (e) Absolute value as $QABS$ (f) The two's complement of signed binary integer as QTC (adapted from [3], [19]).

3. Algorithm of Quantum Image Mean Filtering with Different Sized

In this section, algorithm of quantum image mean filtering with different sized (size as $s \times s$) based on the NEQR model is presented. The stages of the algorithm and the quantum circuits designed for the stages of the algorithm are presented in detail. Some of the presented circuits in this section have an intermittent between the input and output wires of the black-box circuits. This intermittent between the wire is to indicate that the black-box circuit is not applied to the input qubit on that wire.

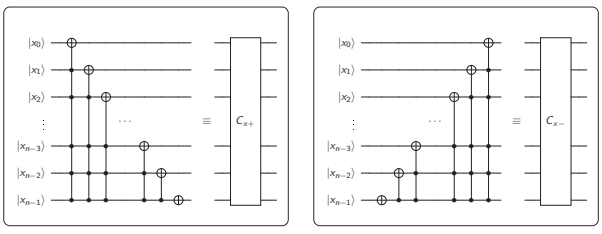

Figure 5. The quantum circuits of the cyclic shift transformation operators on the x-axis (a) C_{x+} (b) C_{x-} (adapted from [20]).

The mean filter operators of sizes 3×3, 5×5 and 7×7 used in this study are as follows.

$$\frac{1}{9}\times\begin{bmatrix}1&1&1\\1&1&1\\1&1&1\end{bmatrix},\frac{1}{25}\times\begin{bmatrix}1&1&1&1&1\\1&1&1&1&1\\1&1&1&1&1\\1&1&1&1&1\\1&1&1&1&1\end{bmatrix}$$

$$\frac{1}{49}\times\begin{bmatrix}1&1&1&1&1&1&1\\1&1&1&1&1&1&1\\1&1&1&1&1&1&1\\1&1&1&1&1&1&1\\1&1&1&1&1&1&1\\1&1&1&1&1&1&1\\1&1&1&1&1&1&1\end{bmatrix}. \quad (8)$$

The algorithm for applying the $s\times s$ mask filter operator to the $2^n\times2^n$ sized NEQR image ($|I\rangle$) with q-bit color depth (2^q gray-scale) is given in Algorithm 1.

The division operations in the algorithm are integer division operations, so division results are integer.

The quantum state $|I_N\rangle$ with color states $|0\rangle^{\otimes q}$ for the noiseless NEQR image is prepared as in (9) as follows.

$$|I_N\rangle=\frac{1}{2^n}\sum_{y=0}^{2^n-1}\sum_{x=0}^{2^n-1}|0\rangle^{\otimes q}|yx\rangle. \quad (9)$$

According to the size of the mask filter operator to be applied, the neighboring pixels of the y and $x<=(s/2)-1^{th}$ and y and $x>=2^n-(s/2)^{th}$ rows and columns are missing. Therefore, the operator is not applied for those pixels, and the corresponding pixel value is taken exactly from $|I\rangle$ to $|I_N\rangle$ by applying the operation U_C.

First, the quantum state $|V_{yx}\rangle$ is prepared in the initial state of r-qubits (where $r=log_2(2^q\times s^2)$) for the maximum value of the $|V_{yx}\rangle$ and the quantum state $|Vf_{yx}\rangle$ is prepared in the initial state of q-qubits for the result of the division result. For the corresponding pixel (y,x) and its neighboring pixels, the value of the pixel $(0,0)$ of the image is added to the variable $|V_{yx}\rangle$ by applying the operation $QNMAdd$. The next pixel in the image is moved to the position $(0,0)$ by using the cyclic shift transformation operators [20], then the pixel at position $(0,0)$ is added to $|V_{yx}\rangle$ by applying the operation $QNMAdd$. This process is repeated for all relevant pixels according to the size $(s\times s)$ of the

Algorithm 1: Applying the filter mask operator to the NEQR image

Input: $|I\rangle$: The NEQR image, s: Filter operator size
Output: $|I_N\rangle$: The noiseless NEQR image

```
begin
    Prepare the state |I_N⟩ with color states |0⟩^{⊗q} for noiseless NEQR image
    for y ← 1 to 2^n − 1 by 1 do
        for x ← 1 to 2^n − 1 by 1 do
            if ((y<= (s/2) − 1) or (y>= 2^n − (s/2)) or (x<= (s/2) − 1) or (x>= 2^n − (s/2))) ) then
                Assign the color value of the image |I_(y,x)⟩ to the color value of the image |I_{N_(y,x)}⟩ by using the yx-controlled U_C operation
            else
                Calculate the value |Vf_yx⟩ for the corresponding pixel by applying the circuit QV_yx to the |I⟩
                Assign |Vf_yx⟩ to the color value of the image |I_{N_yx}⟩
```

mask operator. Finally, the obtained value $|V_{yx}\rangle$ is divided by the total number of elements in the mask operator by applying the operation $QNMDiv$ and the value of the new pixel is calculated as $|Vf_{yx}\rangle$. The algorithm of this operation as QV_{yx} is given in Algorithm 2. The quantum circuit of the operation QV_{yx} for 3×3 filter operator is shown in Figure 6.

In this study, the cyclic shift transformation operators [20] are used for the shifting process. The quantum circuits of the transformations operators C_{x+} and C_{x-} are shown in Fig. 5. The implementation of the cyclic shift transformations $C_{y\pm}$ on the y-axis and $C_{x\pm}$ on the x-axis for a $2^n \times 2^n$ NEQR image are given in (10) and (11).

$$\begin{aligned} |C_{y\pm}\rangle |I\rangle &= \frac{1}{2^n} \sum_{y=0}^{2^n-1} \sum_{x=0}^{2^n-1} |C_{yx}\rangle \, |(y \pm 1) \; mod \; 2^n\rangle \, |x\rangle \\ &= \frac{1}{2^n} \sum_{y=0}^{2^n-1} \sum_{x=0}^{2^n-1} |C_{y'x}\rangle \, |y\rangle \, |x\rangle \, . \end{aligned} \tag{10}$$

$$\begin{aligned} |C_{x\pm}\rangle |I\rangle &= \frac{1}{2^n} \sum_{y=0}^{2^n-1} \sum_{x=0}^{2^n-1} |C_{yx}\rangle \, |y\rangle \, |(x \pm 1) \; mod \; 2^n\rangle \\ &= \frac{1}{2^n} \sum_{y=0}^{2^n-1} \sum_{x=0}^{2^n-1} |C_{yx'}\rangle \, |y\rangle \, |x\rangle \, . \end{aligned} \tag{11}$$

After calculating the value $|Vf_{yx}\rangle$ for the relevant pixel of the image $|I\rangle$, the value $|Vf_{yx}\rangle$ is assigned to the noiseless image $|I_{N_{yx}}\rangle$ by the yx-controlled U_C operation. The operation C_{x-} is applied to the image $|I\rangle$ and the next pixel in the row is moved to the position $(0, 0)$. The process repeats for all pixels in the relevant row.

According to the size $(s \times s)$ of the mask operator to be applied, when the pixel in the $2^n - (s/2)^{th}$ column is at the position $(0, 0)$, the operation C_{x-} is applied $(s/2) + 1$ times to bring the pixel that was originally at the position $(0, 0)$ to the position

Algorithm 2: Algorithm of the operation QV_{yx}

$r \leftarrow$ Round up$(log_2(2^q \times s^2))$
$|V_{yx}\rangle \leftarrow |0\rangle^{\otimes r}$
$|Vf_{yx}\rangle \leftarrow |0\rangle^{\otimes q}$
for $i \leftarrow 1$ **to** s **by** 1 **do**
  for $j \leftarrow 1$ **to** s **by** 1 **do**
    $|V_{yx}\rangle \leftarrow |V_{yx}\rangle + |I_{(0,0)}\rangle$ // by using the QNMAdd
    if *(j == s)* **then**
      for $k \leftarrow 1$ **to** $(s/2)+1$ **by** 1 **do**
        $C_{x+}\,|I\rangle$ // All the pixels are shifted right $(s/2)+1$ times by the x-axis to their original positions.
    else
      $C_{x-}\,|I\rangle$ // All the elements of the $|I\rangle$ are shifted left by the x-axis. In the first iteration, the pixel (0,1) is moved the position (0,0).
  if *(i == s)* **then**
    for $k \leftarrow 1$ **to** $(s/2)+1$ **by** 1 **do**
      $C_{y+}\,|I\rangle$ // All the pixels are shifted down $(s/2)+1$ times by the y-axis to their original positions.
  else
    $C_{y-}\,|I\rangle$ // All the pixels of the $|I\rangle$ are shifted up by the y-axis. In the first iteration, the pixel (1,0) is moved the position (0,0).
$|Vf_{yx}\rangle \leftarrow |V_{yx}\rangle \,/\, |s^2\rangle$ // by using the QNMDiv

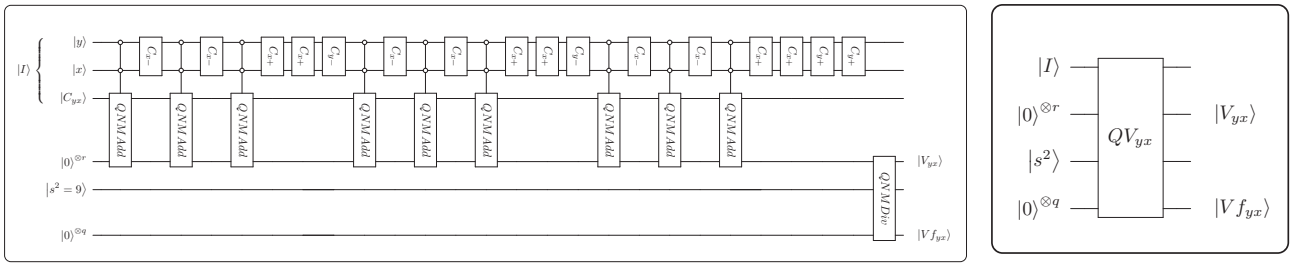

(a) (b)

Figure 6. (a) The quantum circuits of the operation QV_{yx} for 3×3 filter operator (b) simplified graph of QV_{yx}.

$(0, 0)$. Then the operation C_{y-} operation is applied for bringing the bottom row to upper row. When the pixel in the $2^n - (s/2)^{th}$ row and column is at the position $(0, 0)$, the operation C_{y-} is applied $(s/2)+1$ times to bring the pixel that was originally at the position $(0, 0)$ to the position $(0, 0)$. The quantum circuit of applying the mask operator to the whole image as QMF is shown in Figure 7.

4. Complexity and Simulation Analysis

In this section, the circuit complexities of the proposed algorithm and the simulation analysis are presented. Also, the simulation results obtained using noised image by "salt and pepper" filter with density 0.05 and 0.1 and different sized filter mask operator are evaluated.

4.1. Complexity analysis

Considering an $2^n \times 2^n$ image with the color range $[0, 2^q - 1]$ and the $s \times s$ sized mask filter operator as an example ($q + 2n$ qubits required for image), the circuit complexity is analyzed as follows:

The circuit complexity of the preparation of the NEQR quantum image $|I\rangle$ from the classical image is $O(qn2^{2n})$ according to [8]. The $2n$ Hadamard gates are required for preparing the initial state of the noiseless NEQR quantum image $|I_N\rangle$, so the complexity is $O(n)$.

The operation QMF applied to the whole image to obtain a noiseless NEQR image $|I_N\rangle$ consists of the sub-operations as QV_{yx}, controlled U_C, cycling shift transformations $C_{x\pm}$ and $C_{y\pm}$. The operation QV_{yx} consists of (s^2) $QNMAdd$, $(s-1)$ C_{x-}, $(s-1)$ C_{x+}, (s) C_{y-} and one $QNMDiv$ operations. According to [19], the circuit complexities of the operations of $QNMAdd$ with (q, r) qubits inputs and $QNMDiv$ with (r, p) qubits inputs are at most $O(q^2)$ and $O(qp)$, respectively (where $p = log_2(s^2)$, From Algorithm 2 $r \sim q$). The circuit complexities of the cyclic shift transformation operators $C_{x\pm}$ and $C_{y\pm}$ with n qubits inputs are at most $O(n^2)$ for both [20]. The circuit complexities of the operation U_C with q qubits input is at most $O(n)$ for both [19]. As a result, the circuit complexity of the operation QMF will be $O(s^2q^2+sn^2)$ at most. If we consider that s will have 3, 5, 7 values, we can accept the complexity as $O(q^2 + n^2)$.

In quantum image processing studies, the circuit complexity of the preparation of the quantum image from the classical image is high. For the accuracy of the efficiency of the algorithms, this

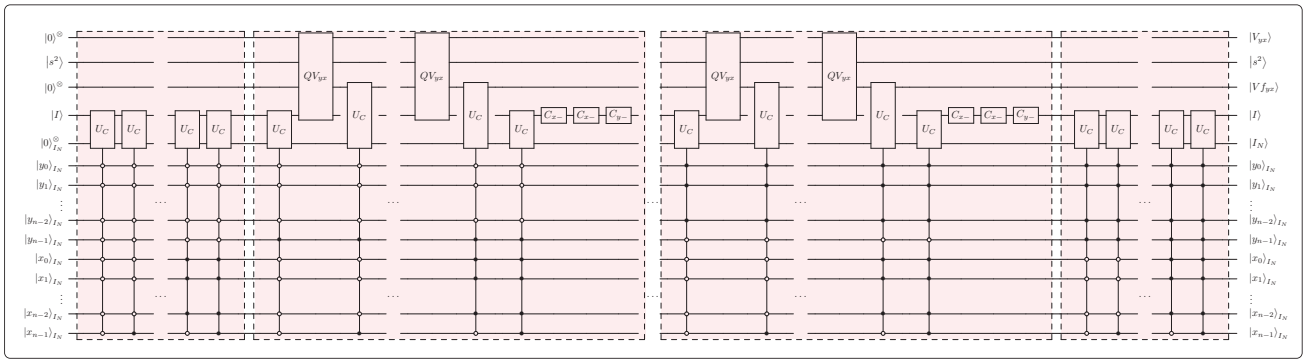

Figure 7. The quantum circuit (QMF) of applying the mask operator to the whole image.

image transformation process is not included in the circuit complexity. Thus, the complexity of the noise removal algorithm in this study is $O(q^2 + n^2)$ at most.

4.2. Quantum simulation resources

The physical quantum hardware is not affordable for us to execute our algorithm; therefore, proposed algorithm is simulated by using the Microsoft Quantum Development Kit and Matlab R2015a with the classic computer INTEL(R) Core(TM) i7-12700 CPU 2.30 GHz, 16GB RAM equipped. In this study, the image with size 512×512 called as "Lena" used as test image, and the versions of "Lena" noised by "salt and pepper" filter with density 0.05 and 0.1 are shown in Figure 8. The images obtained from the 0.05 and 0.1 density noisy images by removing the noise by applying 3×3, 5×5 and 7×7 sized filters are shown in Figures 9 and 10.

(a) (b) (c)

Figure 8. Images used in this simulation (a) original (b) noised by density 0.05 (c) noised by density 0.1.

(a) (b) (c)

Figure 9. The noise reduced images obtained by using filter operators with sized (a) 3×3 (b) 5×5 (c) 7×7 from noise density 0.05 image.

4.2..1 Correlation analysis for adjacent pixels

To measure and compare the correlations of adjacent pixels in the original, noisy and filtered images, the correlation coefficient R_{yx} of adjacent pixels is calculated by (12) [18].

$$R(x,y) = \frac{E((x - E(x)))(y - E(y))}{\sqrt{D(x)D(y)}}. \qquad (12)$$

where $E(x)$ and $D(x)$ represent the expected

(a) (b) (c)

Figure 10. The noise reduced images obtained by using filter operators with sized (a) 3×3 (b) 5×5 (c) 7×7 from noise density 0.1 image.

value and variance of the pixel, respectively. The correlation is tested between two adjacent pixels in horizontally and vertically directions in the original, noisy and filtered images. The correlation between pixels is obtained by randomly selecting 1000 pairs of adjacent pixels in the two directions from the images. Let I_O, $I_{N\_0.05}$, $I_{NF3\_0.05}$, $I_{NF5\_0.05}$, $I_{NF7\_0.05}$, $I_{N\_0.1}$, $I_{NF3\_0.1}$, $I_{NF5\_0.1}$ and $I_{NF7\_0.1}$ represent, respectively, the original image, the noisy image with density 0.05, the filtered images with 3×3, 5×5 and 7×7 filters from noised with density 0.05, the noisy image with density 0.1, the filtered images with 3×3, 5×5 and 7×7 filters from noised with density 0.1. The results of the correlation coefficient are presented in Table 1.

It can be seen from Table 1 that the correlation between adjacent pixels decreases in noisy images. As the noise density increases, the correlation decreases further. The correlation increases after filtering is applied. It is clearly seen that the correlation increases as the size of the applied filter increases.

4.2..2 Visual quality

Peak signal-to-noise ratio (PSNR) is used to describe quantitatively the visual quality of a filtered image [18], [17] and can be written in (13).

Table 1.
Correlation coefficient for horizontal and vertical pairs of adjacent pixels for the original, noisy and filtered images.

Image	Horizontal correlation	Vertical correlation
I_O	0.9669	0.9796
$I_{N\_0.05}$	0.6545	0.6177
$I_{NF3\_0.05}$	0.9711	0.9795
$I_{NF5\_0.05}$	0.9894	0.9920
$I_{NF7\_0.05}$	0.9930	0.9959
$I_{N\_0.1}$	0.4706	0.4476
$I_{NF3\_0.1}$	0.9513	0.9595
$I_{NF5\_0.1}$	0.9848	0.9884
$I_{NF7\_0.1}$	0.9919	0.9939

where I_{OR} and I_{NF} are the original image and the noise (or filtered) image, respectively. The PSNR values for the noisy and filtered images are presented in Table 2.

Table 2.
The PSNR values of the noisy and filtered images.

Image	PSNR (dB)
$I_{N\_0.05}$	18.1818
$I_{NF3\_0.05}$	26.0983
$I_{NF5\_0.05}$	26.3355
$I_{NF7\_0.05}$	25.6109
$I_{N\_0.1}$	15.2771
$I_{NF3\_0.1}$	23.5303
$I_{NF5\_0.1}$	24.8630
$I_{NF7\_0.1}$	24.6594

It can be seen from the PSNR values in Table 2 that the visual qualities of noisy images are poor. If the noise reduction in the image is increased, the blur in the image will increase and the visual quality will decrease. Thus, the visual quality will

$$\text{PSNR} = 20\ log_{10}\frac{255}{\sqrt{\frac{1}{2^{2n}}\sum_{i=0}^{2^n-1}\sum_{j=0}^{2^n-1}[I_{OR}(i,j) - I_{NF}(i,j)]^2}} \tag{13}$$

deteriorate. Simulation results show that the best visual quality is obtained with 5×5 sized filtering.

5. Conclusion

Image filtering is an important operation for image processing. Removing noise in images is also an important step for more efficient results in image processing. Due to the increase in the size of the images and the needed applications, the number of processes and memory requirements increase, so quantum computing methods provide significant advantages in solving problems. In this paper, a new method is proposed that reduces the number of operations and the number of qubits used for quantum mean filtering on quantum images by using QFT-based arithmetic operators. Besides, the effects of using filtering operators of different sizes on images were examined. The efficiency of the method is shown by revealing the circuit complexity of the developed method. The effects of filters of different sizes are also revealed by simulation results. The efficiency of classical algorithms is evaluated in terms of time complexity by considering commands in high-level languages. The efficiency of quantum algorithms is evaluated by the circuit complexity based on the number of one and two qubit elementary gates used in the circuit of the method. Therefore, it would not be very accurate to compare classical and quantum methods. However, on the basis of the superposition and entanglement principles of quantum computing, when we consider that a single operator operates simultaneously in all possible states, it is clear that quantum methods have a significant advantage over classical methods in terms of both speed and memory.

The proposed method will contribute to the more efficient implementation of other noise removal and different filtering processes. Investigation of the use of QFT-based operators in different quantum image representation models for frequency filtering other than spatial filtering will be our next research topic.

Acknowledgments

We would like to thank referees for valuable suggestions.

References

[1] T.D. Ladd, F. Jelezko, R. Laflamme, Y. Nakamura, C. Monroe, and J.L. OBrien, *Quantum computers*, Nature, vol. 464, no. 7285, pp. 45, 2010.

[2] M. Mandviwalla, K. Ohshiro and B. Ji, *Implementing Grover's algorithm on the IBM quantum computers*, In Proceedings of the 2018 IEEE International Conference on Big Data, Seattle, WA, USA, pp. 2531–2537, 2018.

[3] E. Şahin, *Implementation of addition and subtraction based on quantum Fourier transform on IBM quantum computer*, In Proceedings of the 2nd International Symposium of Scientific Research and Innovative Studies, Bandirma, Balikesir, Turkey, pp. 593–605, 2022.

[4] M. A. Nielsen, and I. L. Chuang, *Quantum Computation and Quantum Information: 10th Anniversary Edition*. Cambridge University Press, New York, NY, USA, 2011.

[5] E. Şahin, and I. Yilmaz, *A quantum edge detection algorithm for quantum multi-wavelength images*, Int. J. Quantum Inform., vol. 19, no. 3, 2150017, 2021.

[6] P. Q. Le, F. Dong, and K. Hirota, *A flexible representation of quantum images for polynomial preparation, image compression, and processing operations*, Quantum Inf. Process., vol. 10, pp. 63–84, 2011.

[7] B. Sun, A. Iliyasu, F. Yan, F. Dong, and K. Hirota, *An RGB multi-channel representation for images on quantum computers*, J. of Adv. Comp. Intelligence and Intelligent Informatics, vol. 17, no. 3, pp. 404–417, 2013.

[8] Y. Zhang, K. Lu, Y. Gao, and M. Wang, *A novel enhanced quantum representation of digital images*, Quantum Inf. Process., vol. 12, no. 8, pp. 2833–2860, 2013.

[9] J. Z. Sang, S. Wang, and Q. Li, Q. *A novel quantum representation of color digital images*, Quantum Inf. Process., vol. 16, pp. 14, 2017.

[10] E. Şahin, and İ. Yilmaz, *QRMW: quantum representation of multi wavelength images*, Turk. J. Electr. Eng. Comput. Sci., vol. 26, no. 2, pp. 768–779, 2018.

[11] J. Su, X. Guo, C. Liu and L. Li, *A new trend of quantum image representations*, IEEE Access, vol. 8, pp. 214520–214537, 2020.

[12] S. Jiang, R. G. Zhou, W. Hu, and Y. Li, *Improved quantum image median filtering in the spatial domain*, Int. J. Theor. Phys., vol. 58, pp. 2115–2133, 2019.

[13] C. Lomont, *Quantum convolution and quantum correlation algorithms are physically impossible*, arXiv preprint arXiv:quant-ph/0309070, 2003.

[14] S. Yuan, X. Mao, J. Zhou, and X. Wang, *Quantum image filtering in the spatial domain*, Int. J. Theor. Phys., vol. 56, no. 8, pp. 2495–2511, 2017.

[15] S. Yuan, Y. Lu, X. Mao, Y. Luo, and J. Yuan, *Improved quantum image filtering in the spatial domain*, Int. J. Theor. Phys., vol. 57, no. 3, pp. 804–813, 2018.

[16] P. Li, X. Liu, and H. Xiao, *Quantum image weighted average filtering in spatial domain*, Int. J. Theor. Phys., vol. 56, no.11, pp. 3690–3716, 2017.

[17] P. Li, X. Liu, and H. Xiao, *Quantum image median filtering in the spatial domain*, Quantum Inf. Process., vol. 17, no. 3, pp. 49, 2018.

[18] A. E. Ali, H. Abdel-Galil, and S. Mohamed, *Quantum image mid-point filter*, Quantum Inf. Process., vol. 19, pp. 238, 2020.

[19] E. Şahin, *Quantum arithmetic operations based on quantum Fourier transform on signed integers*, Int. J. Quantum Inform., vol. 18, no. 6, 2050035, 2020.

[20] P. Q. Le, A. M. Iliyasu, F. Dong and K. Hirota, *Strategies for designing geometric transformations on quantum images*, Theor. Comput. Sci., vol. 412, no. 15, pp. 1406–1418, 2011.